

STEADY-STATE CENTRIFUGAL INPUT VIA THE LATERAL OLFACTORY TRACT MODULATES SPONTANEOUS ACTIVITY IN THE RAT MAIN OLFACTORY BULB

NEIL C. FORD * AND EDWIN R. GRIFF

Department of Biological Sciences, University of Cincinnati,
P.O. Box 210006, Cincinnati, OH 45221, USA

Abstract—Mitral and tufted cells in the main olfactory bulb (MOB) of anesthetized rats exhibit vigorous spontaneous activity, action potentials produced in the absence of odor stimuli. The central hypothesis of this paper is that tonic activity of centrifugal input to the MOB modulates the spontaneous activity of MOB neurons. The spontaneous activity of centrifugal fibers causes a baseline of steady-state neurotransmitter release, and odor stimulation produces transient changes in the resulting spontaneous activity. This study evaluated the effect of blocking centrifugal axon conduction in the lateral olfactory tract (LOT) by topically applying 2% lidocaine. Mean spontaneous activity of single bulbar neurons was recorded in each MOB layer before and after lidocaine application. While the spontaneous activity of most MOB neurons reversibly decreased after blockade of the LOT, the spontaneous activity of some neurons in the mitral, tufted and granule cell layers increased. The possible mechanisms producing such changes in spontaneous activity are discussed in terms of the tonic, steady-state release of excitatory and/or inhibitory signals from centrifugal inputs to the MOB. The data show for the first time that tonic centrifugal input to the MOB modulates the spontaneous activity of MOB interneurons and projection neurons. The present study is one of the few that focuses on steady-state spontaneous activity. The modulation of spontaneous activity demonstrated in this study implies a behaviorally relevant, state-dependent regulation of the MOB by the CNS. © 2017 IBRO. Published by Elsevier Ltd. All rights reserved.

Key words: main olfactory bulb, lateral olfactory tract, spontaneous activity, centrifugal input.

INTRODUCTION

The mammalian main olfactory bulb (MOB) receives sensory input from the olfactory epithelium. The MOB is also innervated by numerous centrifugal fibers that originate from neuromodulatory nuclei and cortices (Price and Powell, 1970a,b,c; Davis and Macrides, 1981; Zaborszky et al., 1986; Matsutani and Yamamoto, 2008; Matsutani, 2010). Output neurons from the MOB reciprocally innervate the cortical sources of centrifugal fibers (Nagayama et al., 2010). For example, mitral and tufted cell projections target the piriform cortex, which contains neurons that extend projections back to the MOB, synapsing onto mitral and tufted cells as well as inhibitory networks within the bulb (Ennis et al., 2007; Matsutani and Yamamoto, 2008; Matsutani, 2010; Markopoulos et al., 2012).

Centrifugal fibers also originate from brain nuclei located in the basal forebrain, reticular formation, and pons, which do not receive olfactory signals from the MOB (Zaborszky et al., 1986; McLean and Shipley, 1987; Jiang et al., 1996; Matsutani and Yamamoto, 2008). Neuromodulatory fibers form synapses throughout the MOB (Price and Powell, 1970a,b; Zaborszky et al., 1986; Ennis et al., 2007) and release norepinephrine, serotonin, GABA, and acetylcholine (Zaborszky et al., 1986; Pompeiano et al., 1994; Jiang et al., 1996) into the MOB. The neuromodulatory effects of these neurotransmitters include elevating the excitability of mitral cells (Ciombor et al., 1999), modulating sensitivity, contrast, and synchronization of olfactory signal perception (Devore and Linster, 2012), regulating olfactory learning and olfactory memory (Fletcher and Chen, 2010), and maintaining olfactory circuits (Leo and Brunjes, 2003; Ennis et al., 2007; Ennis and Hayar, 2008; Matsutani and Yamamoto, 2008).

Cortical and neuromodulatory centrifugal fibers reach the MOB via two distinct pathways. The largest, termed the extrinsic centrifugal fiber projection by Laaris et al., 2007, is clearly differentiated from the lateral olfactory tract (LOT), and includes fibers from the anterior olfactory nucleus (AON), anterior commissure, and medial forebrain bundle (Ennis, personal communication). More than half of the centrifugal fibers to the MOB project through the AON (Carson, 1984), and the majority of these centrifugal fibers originate from primary olfactory cortices (Matsutani and Yamamoto, 2008; Matsutani, 2010; Markopoulos et al., 2012). However, the LOT also

*Corresponding author at: Department of Anesthesiology, University of Cincinnati College of Medicine, 231 Albert Sabin Way, Cincinnati, OH 45267, USA.

E-mail address: fordnc@mail.uc.edu (N. C. Ford).

Abbreviations: ACSF, artificial cerebral spinal fluid; AON, anterior olfactory nucleus; EPL, external plexiform layer; GCL, granule cell layer; GL, glomerular layer; HDB, horizontal limb of the diagonal band of Broca; Hz, hertz; LOT, lateral olfactory tract; MCL, mitral cell layer; MOB, main olfactory bulb; ON, olfactory nerve; ONL, olfactory nerve layer.

contains centrifugal fibers originating from olfactory cortices as well as the horizontal limb of the diagonal band of Broca (HDB) (Price and Powell, 1970b; Pinching and Powell, 1972; Davis and Macrides, 1981; Zaborszky et al., 1986; Niedworok et al., 2012). The HDB contains both cholinergic and GABAergic neurons (Zaborszky et al., 1986; Jeune et al., 1995; Niedworok et al., 2012), and thus, potentially supplies excitatory and inhibitory influences to bulbar neurons.

Most of what is known about the functions of centrifugal input to the MOB comes from electrophysiological and behavioral studies where centrifugal fibers or their sources are stimulated, and from studies that examine the effects of blocking or ablating centrifugal inputs (Inokuchi et al., 1987; Jiang et al., 1996; Kiselycznyk et al., 2006; Ma and Luo, 2012; Markopoulos et al., 2012). These studies demonstrate that centrifugal input shapes bulbar activity in response to stimulation and effects odorant-related behaviors. However, these studies provide less information about the impact of centrifugal input in the absence of stimulation. Reducing centrifugal fiber input in the LOT has been shown to alter local field potentials in the MOB (Gray and Skinner, 1988). Prior studies have demonstrated that certain brain nuclei such as the HDB and the locus coeruleus are active at rest (Jiang et al., 1996; Linster and Hasselmo, 2000). These studies suggest that some centrifugal fibers are active without any imposed stimulation. However, the degree to which tonic centrifugal fiber activity modulates the spontaneous activity of individual MOB neurons remains largely unknown.

The present experiments examine the effects of steady-state centrifugal fiber input on the spontaneous activity of single units in the MOB. Spontaneous activity in sensory networks contributes to the background activity over which sensory signals must be detected, thereby setting the signal-to-noise ratio. Spontaneous activity also increases the dynamic range of sensory circuits so that responses can be represented as increases or decreases in activity (Chaput et al., 1992). The neurochemical environment of the MOB in its resting steady state is likely determined by tonic release of neurotransmitters from spontaneously active MOB neurons and the release of neurotransmitters from active centrifugal fibers. The spontaneous activity of mitral and tufted cells, in turn, contributes to the neurochemical environment of the central olfactory structures to which they project (Brunjes et al., 2005).

While the levels of spontaneous activity in the MOB *in vivo* have been reported to be quite robust, *in vitro* preparations of MOB slices, after denervation of sensory and centrifugal fibers, still exhibit low levels of spontaneous activity. Although centrifugal fiber activity is clearly not the only source of modulatory influences on bulbar neurons, it remains unclear to what extent steady-state centrifugal input contributes to their spontaneous activity. Therefore, the present study identifies tonic centrifugal fiber input to the MOB as a

key regulator of spontaneous activity of bulbar neurons *in vivo*.

EXPERIMENTAL PROCEDURES

Ethical approval

Experimental procedures were conducted in agreement with the Institutional Animal Care and Use Committee (IACUC) protocol 10-05-20-01 at the University of Cincinnati. The experimental methods utilized in this study have been described in prior reports (Nica et al., 2010; Stakic et al., 2011) and are only briefly described below. Twenty-nine male Sprague–Dawley rats (Charles River Laboratories; Wilmington, Massachusetts) ranging in weight from 205 to 442 g were used in this study. The animals were housed with a 12-h light/dark cycle with access to food and water *ad libitum*. Anesthesia was provided prior to surgical procedures by an intraperitoneal injection of 4% chloral hydrate at the initial loading dose of 400 mg/kg (10 ml/kg). Animals were additionally implanted with an I.P. catheter so that additional anesthesia could be administered as needed. Although anesthetic drugs can alter spontaneous activity (Jiang et al., 1996; Rinberg et al., 2006), the specific anesthetic protocol was designed to minimize such effects. A surgical plane of anesthesia was maintained throughout the preparation of the animals for recording sessions. Parietal cortex EEGs were closely monitored to ensure appropriate levels of anesthesia. For electrophysiological recordings, the plane of anesthesia was maintained such that a hard toe pinch failed to elicit a reflexive withdrawal response, but desynchronized the EEG. Respiratory rate was also closely monitored as an additional measure of the depth of anesthesia. Lidocaine was applied to surgical wounds to provide local anesthesia. Animals were placed on a heat pad so that animal body temperature could be maintained at 37 ± 0.5 °C.

Surgical preparation

Exposure of the dorsal aspect of the MOB was accomplished by removing part of the frontal bone. The LOT was then exposed by removing the lateral aspect of the temporal bone. In some experiments, olfactory nerve (ON) bundles were exposed by removing the caudal portion of the nasal bone. A reference electrode was inserted into the muscles of the neck. The LOT, MOB, and ON were occasionally wetted with artificial cerebral spinal fluid (ACSF) which contained (in mM): 126 NaCl, 25 NaHCO₃, 5.0 glucose, 1.25 NaH₂PO₄-H₂O, 2.5 KCl, 1.0 MgCl, 2.0 CaCl₂.

Positioning of stimulation electrodes

To evoke field potentials used to estimate recording electrode depth, determine the efficacy of lidocaine blockade, and assess the integrity of specific pathways following application of lidocaine (detailed below), one bipolar stainless steel electrode was positioned to contact the ventral LOT where the tract is most

condensed. In some experiments a second LOT stimulation electrode was positioned a few millimeters more rostral on the LOT. Another stimulation electrode contacted the ON rostral to the cribriform plate when that area was exposed or the olfactory nerve layer (ONL) at the rostral end of the exposed MOB. A final stimulation electrode was stereotaxically implanted into the contralateral AON (in mm, from bregma): 4.2 anterior, 2.0 lateral, 4.0 ventral (Paxinos and Watson, 1998). Fig. 1 shows electrode positions. Square wave current pulses (LOT stimulation: 100–1000 μ A, 10–40 μ s; ON/ONL stimulation: (ON) 200–1000 μ A, 750–1000 μ s; AON stimulation: 400–500 μ A, 2 ms) were delivered by a stimulator (Grass Medical Technologies S44, Quincy, MA, USA) through stimulus isolation units (Grass Medical Technologies SIU15, Quincy, MA, USA).

Measurement and analysis of respiratory entrainment

Respirations and single-unit activity were recorded simultaneously. A displacement transducer (Thornton Associates, Inc., Type 424, Waltham, MA, USA) was placed on the lateral most side of the abdomen.

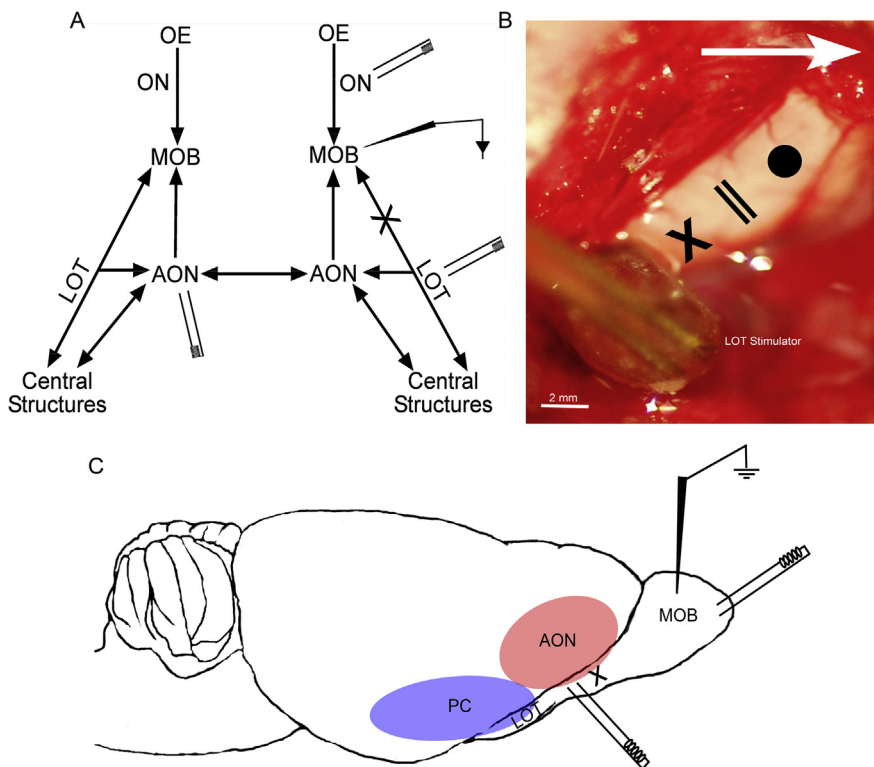


Fig. 1. Position of recording and stimulation electrodes for extracellular recordings of spontaneous activity, field potentials, and compound action potentials. A. Simplified schematic of the olfactory pathway (OE to MOB to central structures) and centrifugal connections (central structures to MOB) demonstrating the placement of a recording electrode in the MOB and stimulation electrodes on the ON, LOT and AON. The black “X” indicates the placement of the lidocaine soaked cotton ball in contact with the LOT. B. Image of recording preparation showing the placement of stimulation and recording electrodes on the LOT for recording compound action potentials. “X”, lidocaine application site. Black filled circle, stainless steel recording electrode for compound action potential recordings. Black lines, second bipolar stimulation electrode. The standard caudal bipolar stimulation electrode embedded in epoxy is visible and labeled. White arrow, rostral direction. C. Anatomical schematic depicting the placement of recording and stimulation electrodes in the MOB and LOT in relation to the anterior olfactory nucleus (red, AON) and piriform cortex (blue, PC). Lidocaine application site (black “X”).

Abdominal movements corresponding to each respiratory cycle were acquired in the Spike2 (Cambridge Electronics Design, CED, Cambridge, England) as a waveform. Respiratory signals were filtered with a band-pass digital filter between 1 and 6 Hz, smoothed, and the beginning of inspiration marked. The subsequent mark represents the end of the expiratory phase and beginning of the next inspiratory phase (360°). Using Spike2, phase correlation histograms were then constructed using these phase markers to correlate occurrences of spikes within each respiration (Fig. 2B). Spikes were put into 50 bins with each bin representing 7.2° (20 ms) each. Angular spike occurrence data were then used in subsequent analysis to determine respiratory entrainment (see Statistics). Rose plots were constructed using MATLAB (r2015a, MathWorks, Inc., Natick, MA, USA).

Single-unit and field potential recordings

Single-unit activity was recorded with glass microelectrodes constructed from thin-walled glass pipettes (1.0 mm outer-diameter, World Precision Instruments; Sarasota, FL USA). Electrode solution was composed of 2% pontamine sky blue dye in sodium acetate solution. Tip diameters ranged from 1.5 to 3.0 μ m. Microelectrodes were inserted randomly into areas of the dorsal MOB where surface blood vessels were minimal. For each unit the microelectrode’s vertical position was adjusted (David Kopf Instruments model 650 Micropositioner; Tujunga, CA, USA) so that the action potential amplitude was maximized. Action potentials were visualized on an oscilloscope (Tektronix model 5111A, Beaverton, OR, USA) and listened to via an audio monitor (Dagan model 2400A, Minneapolis, MN, USA). The following criteria ensured that the recorded action potentials were from a single unit and suitable for recording: (1) consistent action potential amplitude and waveform with the exception of bursting units, where the amplitude typically decreased throughout the burst; (2) inter-spike intervals greater than 2 ms; and (3) baseline rate stability (see below).

Single-unit spontaneous activity and field potentials were recorded at the same location in MOB. All recorded signals were amplified (Dagan model 2400A, Minneapolis, MN, USA), digitized (Cambridge Electronic Design Model micro 1401,

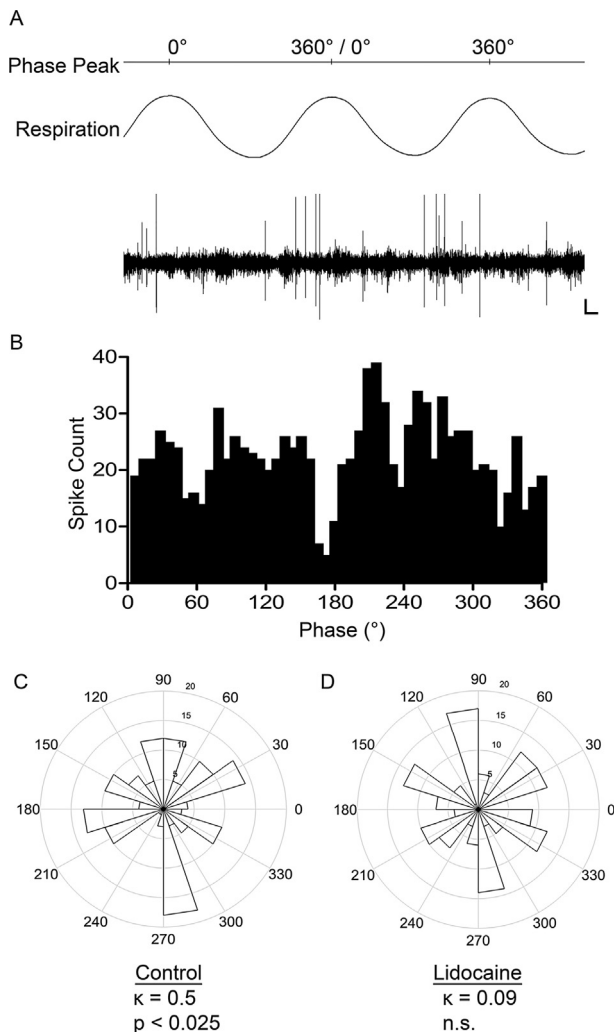


Fig. 2. Respiratory phase determination and spike entrainment analysis. **A.** Representative MOB unit recording showing phase peak marks, the smoothed respiration signal and spike trains. Scale bars: 10 μ V, 0.2 s. **B.** Phase histogram of spike distribution within one respiratory phase (0–360°). **C.** Rose plots of unit spike entrainment with respiration before and after lidocaine where spike entrainment was reduced by LOT blockade. Significant unit entrainment determined by resultant range of p -values < 0.05 after Kuiper's tests of circular uniformity and kappa (κ) estimates (> 0.3) of spike correlation with the mean angular direction of spike distribution.

Cambridge, England) and processed in Spike2. Field potential recordings were band-pass filtered between 0.3 Hz and 3 kHz. Single-unit recordings were band-pass filtered between 30 Hz and 3 kHz. Measurements of the field potentials were taken from either the maximum or minimum of the signal with respect to the baseline. For all recordings, medical grade breathing air was directed past the nares at approximately 0.5 l/min. The air was also purified with activated charcoal and a filter (Alltech Associates, Inc. Deerfield, IL, USA) and humidified before reaching the nares.

At the beginning of each recording, after unit isolation, 5 control field potentials were recorded by stimulating the ventral LOT followed by 5 field potentials recorded from ON or ONL stimulation. The field potential recordings

were followed by a baseline recording of spontaneous activity. In some experiments field potentials were evoked from the AON instead of the ONL or ON so that the integrity of the centrifugal fibers originating in the AON could be monitored. Lidocaine was then used to inhibit centrifugal fibers in these experiments, and was selected for use based on its well-documented efficacy as a nerve block, potential selectivity for voltage-gated sodium channels, and reversibility (Omana-Zapata et al., 1997; Persaud and Strichartz, 2002; Lai et al., 2004).

Lidocaine application

2% lidocaine was topically applied to the LOT under visual control using a small cotton ball soaked with $\sim 2 \mu$ L of lidocaine solution. The elapsed time between control field potentials and lidocaine application ranged from 47.03 to 448.74 s with an average of 165.2 s, and the control ratemeter recordings were made during this time. The lidocaine remained in contact with the LOT for an average of 362 s (range 167–1121 s). The two longest application times, (1121 & 789 s) were due to difficulty in placing the small lidocaine ball in contact with the LOT. Field potentials were evoked by test stimuli to the LOT caudal to the lidocaine application site after 2–3 min to assess when the LOT had been blocked. After the LOT was blocked, 5 field potentials were evoked from the stimulation electrodes to assess the extent of LOT blockade and the potential spread of the lidocaine. Field potentials were evoked from the AON, ON, or ONL of rostral MOB just after the LOT block was measured and these field potentials were used to assess the spread of the lidocaine for each unit. Ratemeter recordings with lidocaine were made after determination of the lidocaine blockade. The LOT was then rinsed with ACSF to remove the lidocaine. Following a recovery period, 5 additional field potentials were recorded to confirm recovery of the LOT from the lidocaine blockade. In several experiments, a cotton ball saturated with ACSF was applied to the LOT as a control. The ACSF did not significantly change the spontaneous activity (see Fig. 5C).

After completing the recording protocols, dye was iontophoresed into the recording site for later recovery of the position of the electrode tip. No more than 3 dye markings were left in any one animal. Animals were then perfused with 10% neutral-buffered formalin; brains were collected and stored in a solution containing 10% neutral-buffered formalin and 20% sucrose for at least two days before sectioning. Frozen brains were then sectioned at 30- μ m thickness using a sliding microtome. Neutral red counterstain was used to visualize MOB layers and to provide contrast for dye spot visualization.

Unit analysis

The average of each set of 5 field potentials (before, during and after lidocaine) was used to evaluate the lidocaine block of the LOT, the potential spread of lidocaine as judged by ON- or ONL-evoked field potentials, and the possible spread of the lidocaine to

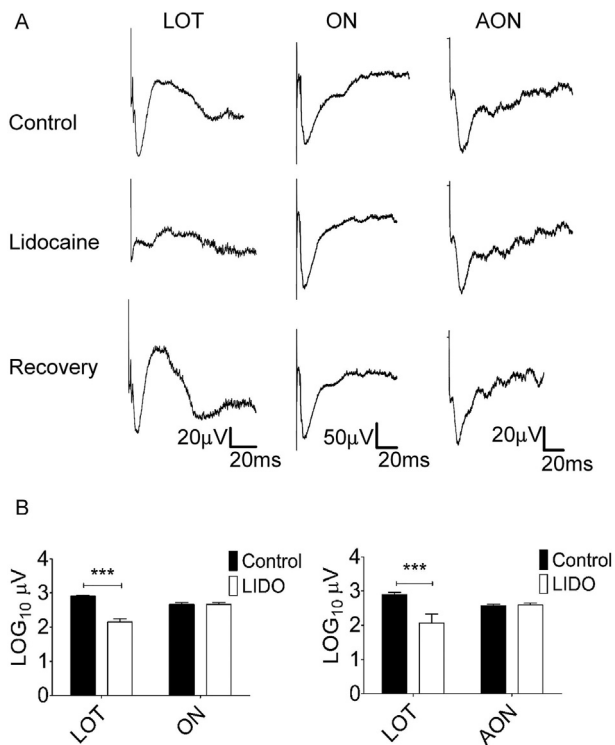


Fig. 3. Topical lidocaine application selectively and effectively blocks LOT-evoked field potentials. **A.** Field potentials recorded from the MOB. Left panel, LOT-evoked field potentials before lidocaine application (top row), after lidocaine (middle row), and after recovery from lidocaine (bottom row). Middle panel, olfactory nerve (ON)-evoked field potentials before, after and recovery from lidocaine. Right panel, anterior olfactory nucleus (AON)-evoked field potentials before, after and recovery from lidocaine. The LOT-evoked field potential was blocked by lidocaine (left panel, middle), while no other field potentials were significantly affected. LOT- and ON-evoked field potential recordings were performed in the same animal, while the AON-evoked field potential was recorded in a separate animal while maintaining the same lidocaine application protocol. **B.** Left panel, assessment of lidocaine spread to the MOB by comparing LOT-evoked vs. ON-evoked field potentials before and after LOT block; a two-way ANOVA revealed a significant interaction between the LOT block and stimulation region $F(1,166) = 31.7, p < 0.001$. LOT block caused a significant decrease in the LOT-evoked field potential, $t = 8.56, p < 0.001$ (Holm–Sidak) but not in the ON-evoked field potential, $t = 0.019, p > 0.05$. Right panel, assessment of lidocaine spread to the underlying AON by comparing LOT-evoked vs. AON-evoked field potentials before and after LOT block. A two-way ANOVA revealed a significant interaction between LOT block and stimulated region $F(1,40) = 9.39, p = 0.004$; LOT-evoked field potential was significantly reduced after LOT block, $***, \alpha = 0.05, t = 4.18, p < 0.001$ (Holm–Sidak), while AON-evoked field potentials were not significantly affected, $t = 0.16, p > 0.05$.

the AON. If field potentials from LOT stimulation were inhibited less than 35%, the recordings were not used in further analyses. Spontaneous activity rates were also measured before and after LOT block (following the control field potential recording, and after lidocaine-dependent decrease of LOT-evoked field potentials), and after the LOT-evoked field potential recovered following ACSF rinse of the LOT to remove the lidocaine. The coefficient of variation (CV) of the interspike intervals was calculated to compare the temporal pattern of the single-unit activity before and during

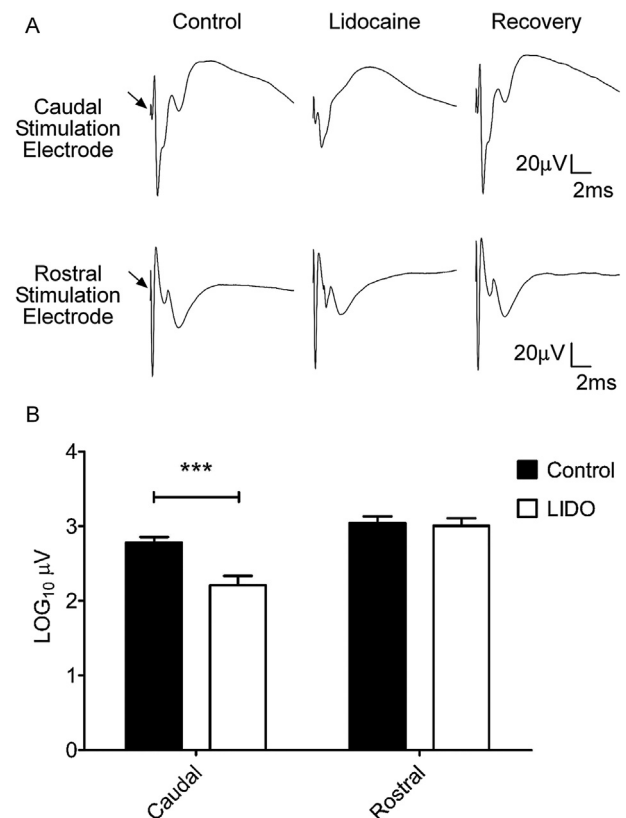


Fig. 4. Topical lidocaine application remains localized to the application site. **A.** Top row, compound action potentials evoked from the caudal LOT stimulation electrode. Bottom row, compound action potentials evoked from the rostral LOT stimulation electrode. Left panel, before lidocaine; middle panel, after lidocaine; right panel, after recovery from lidocaine. The middle panel shows that the lidocaine blocked conduction of the compound action potential evoked from the caudal LOT stimulation electrode, but not from the rostral LOT stimulation electrode. Black arrows, stimulus artifacts. See text for details. **B.** Assessment of lidocaine spread up the LOT by comparing compound action potentials evoked from a caudal stimulator vs. rostral stimulator before and after LOT block. A two-way ANOVA revealed a significant interaction between stimulator position and LOT block, $F(1,44) = 7.39, p = 0.009$; LOT block caused a significant reduction in amplitude of compound action potentials, $***, \alpha = 0.05, t = 4.09, p < 0.001$ (Holm–Sidak), but no significant differences in the amplitude of compound action potentials evoked from the rostral stimulator, $t = 0.25, p = 0.85$.

lidocaine application. Changes in respiration entrainment were assessed by constructing respiratory correlation histograms.

Baseline stability

Assessment of baseline stability began as soon as a unit was isolated while adjusting the electrode position, determining whether the action potentials were from a single unit and whether the unit could be activated antidromically. It was possible to assess baseline stability during these manipulations because we also could listen to the action potentials. After this initial assessment, data recordings began using Spike2. Baseline stability was determined by examining

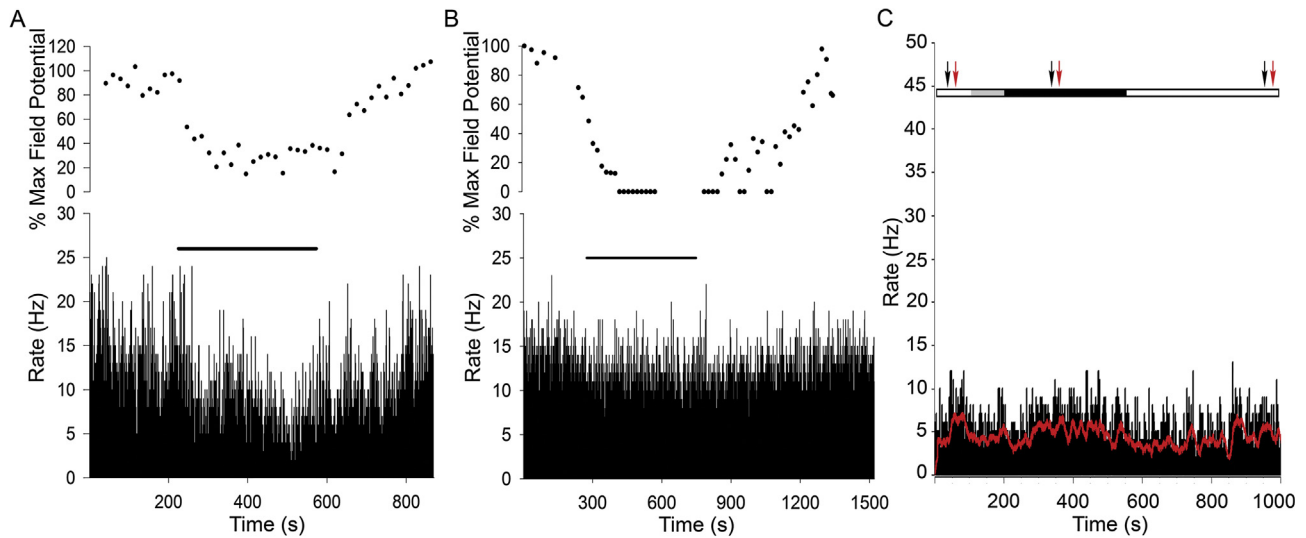


Fig. 5. Time course of changes in LOT-evoked field potentials and baseline stability after lidocaine application. A. Top panel, time course of lidocaine blockade measured as the percent of maximum amplitude of LOT-evoked field potential. Bottom panel, concurrent single-unit recording showing the time course of a reversible decrease in rate due to lidocaine (external plexiform layer). Black bar indicates the time of lidocaine application. B. Top panel, time course of lidocaine blockade measured as percent maximum amplitude of LOT-evoked field potentials. Bottom panel, concurrent single-unit recording showing the time course of a unit's spontaneous activity that did not significantly change due to LOT block (external plexiform layer). Black bar indicates the time of lidocaine application. C. Sample trace of single-unit spontaneous activity showing extended baseline stability (Red trace, rate frequency over 15 s) with pre-baseline (initial White bar), ACSF control (Gray bar), lidocaine application (Black bar), and lidocaine washout (White bar). During the pre-baseline, control field potentials were recorded (Black arrow, LOT-evoked field potentials; Red arrow, ONL-evoked field potentials). At 200 s, the ACSF was removed and lidocaine was applied to the LOT. Around 350 s, field potentials were recorded to determine LOT blockade. At 550 s, lidocaine was removed and LOT was rinsed. Final field potentials were measured at 950 s to assess the recovery of the LOT.

fluctuations in pre-baseline activity (shown only in Fig. 5C) during which control field potentials were also recorded before applying lidocaine and during the recovery period. The mean pre-baseline activity time was 138 ± 70 s and the mean baseline recording time was 166 ± 94 s. The mean recovery time was 416 ± 206 s. In several experiments, a control cotton ball soaked with ACSF was applied to the LOT, and this provided another opportunity to assess baseline stability (see Fig. 5C). The mean time during which the ACSF-soaked ball was in contact with the LOT was 202 s. For every unit, the baseline period started following the control field potentials and ended before the application of lidocaine. Activity in the presence of lidocaine was measured starting immediately after lidocaine application and ending just before removing and rinsing the lidocaine. Fig. 5C shows a sample stable trace of a single unit's spontaneous activity in its entirety: pre-baseline, the timing of control field potentials, ACSF control, baseline before lidocaine, in lidocaine, and after lidocaine washout. Units where it was difficult to determine whether the change following lidocaine application was caused by baseline fluctuations were not used.

Control for spread of lidocaine

In order to determine how far the lidocaine spread from the site of application and to assess the integrity of centrifugal fiber pathways proximal to the LOT after lidocaine application, a bipolar stimulation electrode was positioned in the contralateral AON as described above

(Fig. 1A). AON-evoked field potentials recorded in the MOB were compared before, after, and post-recovery of the LOT. To determine the extent to which lidocaine spreads along the LOT toward the MOB, a second bipolar stimulation electrode was placed on the LOT, rostral to the lidocaine application site (Fig. 1B). A stainless steel recording electrode was positioned rostrally on the LOT (Fig. 1B, black filled circle). Compound action potentials were recorded in the LOT from both stimulation electrodes before and after lidocaine application. Measurements of the compound action potentials were taken from the maximum and minimum of the signal after the stimulus artifact (Fig. 4A, black arrows) and computed as total amplitude.

Statistics

The central hypothesis of this study was that a reduction in tonic centrifugal input through the LOT will alter the rate of spontaneous activity of MOB neurons. Rate measurements taken before and after LOT block were compared using either a two-tailed paired t-test or two-way ANOVA using Holm–Sidak post hoc tests for multiple comparisons. Chi-square analysis was used to determine differential effects of the LOT block between MOB layers. For all statistical tests, a resultant p -value < 0.05 was considered significant. Statistical tests were run using SigmaPlot (Systat Software; San Jose, CA, USA), and Graphpad Prism (Graphpad Software; La Jolla, CA, USA). For all comparisons of both action potential rates and the CV before and following lidocaine blockade, the false discovery rate was

Table 1. Average LOT- and ON-evoked field potentials recorded in each layer of the MOB. Data expressed as mean \pm SEM, for each cell layer in the MOB. ***, $p < 0.001$; n.s., not significant.

Cell Layer	LOT FP Before (μ V)	LOT FP after (μ V)	Mean% Change (μ V)	N	p -Value (LOT)	ON FP before (μ V)	ON FP after (μ V)	Mean% Change (μ V)	N	p -Value (ON)
GL	569.5 \pm 57.5	110.8 \pm 41.8	82.9 \pm 4.7	11	***	471.7 \pm 88.2	460.7 \pm 86.2	6.5 \pm 1.2	10	n.s.
EPL	879.5 \pm 123.9	233.7 \pm 48.8	70.7 \pm 6.4	13	***	605.5 \pm 90	583.3 \pm 90.6	9.6 \pm 1.6	10	n.s.
MCL	956.9 \pm 118	251.8 \pm 36.6	69.6 \pm 4.3	13	***	619 \pm 126	649.36 \pm 128	7.9 \pm 2	10	n.s.
GCL	1260.5 \pm 162	431.8 \pm 82.5	65.8 \pm 6.6	11	***	582.3 \pm 75	610.2 \pm 75.3	7.8 \pm 2.8	7	n.s.

controlled for using the Benjamini–Hochberg method. Adjusted p -values (pFDR) < 0.05 were considered statistically significant. If, after running appropriate tests for normality (Kolmogorov–Smirnov), the data were not found to be normally distributed, logarithmic transformations were sufficient to achieve normality. The rates of single-unit spontaneous activity that were recorded from each MOB layer were grouped by the polarity of change in their spontaneous activity: increase, decrease, or no change. Alterations in mean firing rates after LOT block less than 10% of control rate were considered “no change”.

For the respiratory phase correlation histograms the ‘CircStats’ package (Lund and Agostinelli, 2012) in R (v3.3.1, R Core Team, 2016; Vienna, Austria), Kuiper’s test of uniformity was used to determine the respiratory entrainment of each spike distribution. p -Values < 0.05 indicate a non-uniform distribution and probable respiratory entrainment. Kappa (κ) estimates were calculated to determine the strength of correlation between the distribution of spikes and the mean direction. A large Kappa (> 0.3) indicates a strong correlation with the mean direction, and a non-circular distribution, and a small Kappa (< 0.3) indicates a weaker correlation and a more circular spike distribution. Rose plots were also constructed (see Fig. 2).

RESULTS

The following results are based on the recordings of 49 single units from 29 male Sprague–Dawley rats. Recordings were obtained before, after, and in most cases, after recovery of the LOT from topically applied lidocaine that specifically blocked centrifugal input to the MOB via the LOT.

Topical lidocaine selectively inhibits LOT-evoked field potentials

Evoked field potentials in response to LOT stimulation were used to determine the blockade of centrifugal fiber input to the MOB. Fig. 3A (left panel) shows a representative LOT-evoked field potential that decreased by 94.7% in response to lidocaine application. On average, lidocaine application resulted in the reduction of LOT-evoked field potentials by 71.8 \pm 0.4%.

Evoked field potentials in response to ON or ONL stimulation were used to assess the possible spread of lidocaine to the MOB. Again, field potential measurements were obtained before, after, and post-recovery of the LOT. (Fig. 3A: left and middle panels).

Lidocaine application to the LOT significantly reduced the LOT-evoked field potential, but had no effect on the ON-evoked field potential (Fig. 3B, left panel). Lidocaine application elicited a significant reduction of the LOT-evoked field potentials in each layer (Table 1), while there was no significant effect of LOT block on the ON-evoked field potential in any layer of the MOB.

Due to the inherent possibility that lidocaine application could diffuse through the LOT and deliver off target effects, AON stimulation-evoked field potentials were obtained to identify such effects in response to lidocaine application. This setup examined whether or not the lidocaine spread through the LOT to block the centrifugal fibers that originate in the contralateral AON and reach the ipsilateral MOB by way of the anterior commissure passing the LOT medially (Paxinos and Watson, 1998). If lidocaine had spread to the AON, the pathway generating the AON-evoked field potential would have been disrupted and the field potential amplitude reduced. Lidocaine application selectively blocked the LOT-evoked field potential but did not significantly affect the AON-evoked field potential (Fig. 3A, B, right panels). This indicates that the AON pathway was not disrupted by lidocaine application to the LOT.

LOT-evoked compound action potential recordings were employed to test the potential spread of lidocaine along the LOT and to ensure that lidocaine application remained localized to the application site. This setup tested whether or not the lidocaine application blocked the compound action potential evoked by the caudal LOT stimulation electrode, but not the compound action potential evoked by a rostral stimulation electrode (Fig. 1B). Lidocaine application resulted in a statistically significant, 71% decrease in the compound action potentials evoked by the caudal LOT stimulator, while having no significant effect on the rostral stimulator evoked compound action potentials (Fig. 4). The distance between the rostral and caudal stimulation electrodes of approximately 3 mm, combined with the statistical analysis (Fig. 4B), suggests that the lidocaine spread less than 3 mm from the application site. These field potential and compound action potential analyses demonstrate that the lidocaine application provided a selective and reliable inhibition of the centrifugal fibers contained within the LOT.

Inhibiting centrifugal fiber activity significantly alters spontaneous activity of MOB neurons

Fig. 5A shows an example of the time course of changes in spontaneous activity in relation to changes in LOT-evoked field potentials. The decrease in field potential

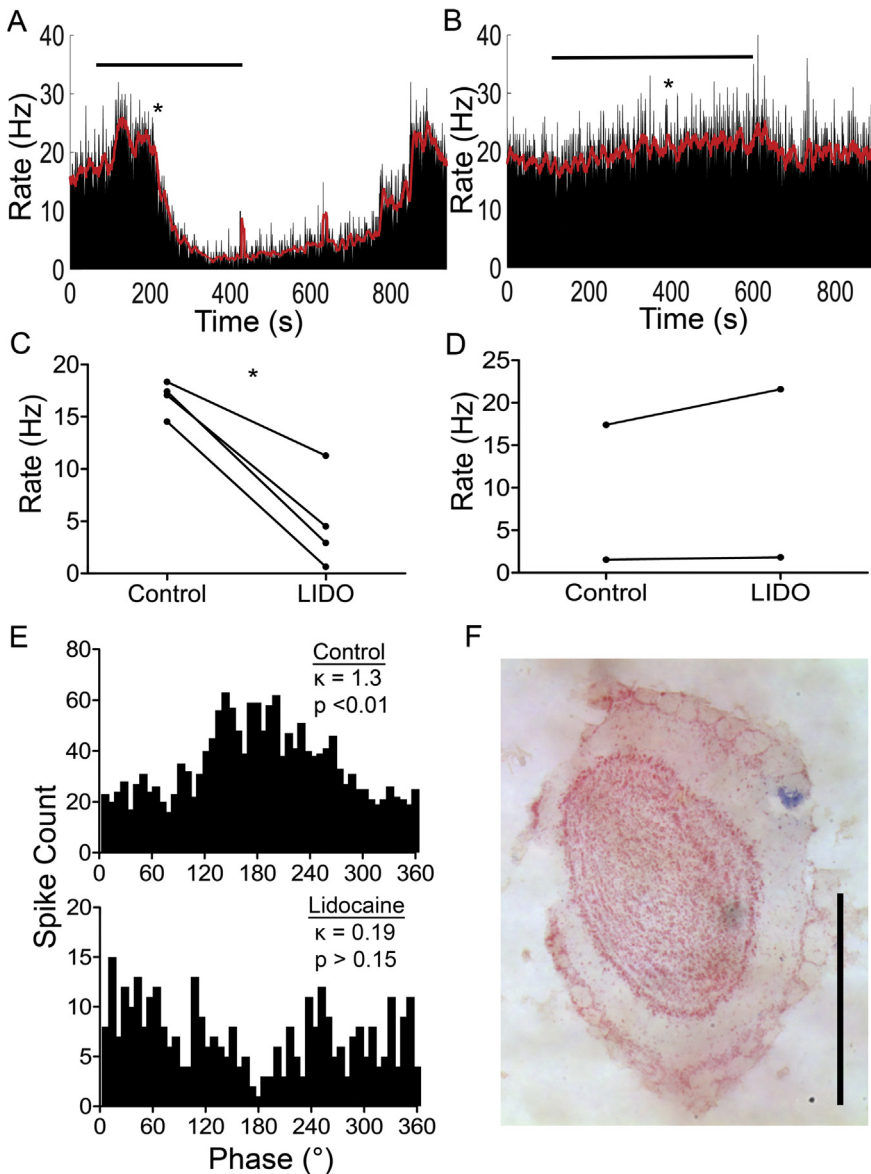


Fig. 6. Tonic activity of centrifugal fibers significantly enhances single-unit spontaneous activity in the glomerular layer. **A.** Representative GL unit ratemeter demonstrating that lidocaine (bar) decreased spontaneous activity from 17.05 Hz to 4.5 Hz, and that baseline rate measurements were stable; red trace overlay, mean rate frequency. LOT was estimated to be maximally blocked around 190 s after lidocaine application, *. **B.** Representative GL unit ratemeter showing that lidocaine (bar) increased spontaneous activity from 17.4 Hz to 21.6 Hz, and that baseline rate measurements were stable; red trace overlay, mean rate frequency. LOT was estimated to be maximally blocked around 400 s after lidocaine application; *. **C.** LOT block significantly decreased the spontaneous activity rate of GL units that were classified as having decreased, pFDR = 0.04. (*, pFDR < 0.05). **D.** Mean increase in spontaneous activity after LOT block of GL units classified as having increased. **E.** Sample phase histograms of a unit in the GL before and after lidocaine application. Top panel, unit activity was significantly entrained with respiration before lidocaine application, $\kappa = 1.3$, $p < 0.01$. Bottom panel, after lidocaine application, unit activity was no longer entrained, $\kappa = 0.19$, $p > 0.15$. **F.** Representative histological determination of recording electrode position in the glomerular layer, blue spot. Scale bar, 1 mm.

amplitude provides a measure of centrifugal fiber inhibition; the time courses of blockade of centrifugal input and the change in spontaneous activity occurred nearly concurrently. Fig. 5B is a representative example of lidocaine completely blocking the LOT-evoked field potential while there was little change in the

spontaneous activity. Even with a nearly complete block of LOT-evoked field potential, the spontaneous activity of some bulbar neurons was not affected by centrifugal fiber inhibition. Note that most experiments were performed without continuous monitoring of the LOT-evoked field potentials; rather, field potentials were only evoked and analyzed before the lidocaine block, after the block reached maximum effectiveness, and after recovery.

Overall, inhibition of centrifugal fibers in the LOT resulted in considerable alterations of the mean spontaneous activity in single units recorded in the glomerular layer (GL; Fig. 6A–D), external plexiform layer (EPL; Fig. 7A–D), mitral cell layer (MCL; Figs. 8A–D), and granule cell layer (GCL; Fig. 9A–D). Lidocaine blockade significantly decreased the mean rate in 4 GL units from 16.8 ± 0.8 Hz to 4.8 ± 2.3 Hz (Fig. 6C, paired t-test, $p = 0.006$, pFDR = 0.04), with an average decrease of $72.7 \pm 12.3\%$; 2 glomerular units increased in mean rate from 9.5 ± 7.9 Hz to 11.7 ± 9.8 Hz (Fig. 6D), with an average increase of $20.5 \pm 3.6\%$; 5 units remained unchanged in response to blocking LOT.

In the EPL, lidocaine blockade decreased the rate of 3 units from 12.1 ± 1.3 Hz to 4.1 ± 2.3 Hz, but did not achieve statistical significance (Fig. 7C, paired t-test, $p = 0.04$, pFDR = 0.09), with an average decrease of $68.2 \pm 15.2\%$. After lidocaine block, 3 units recorded from the EPL increased in mean rate from 9.1 ± 2.8 Hz to 13.8 ± 6 Hz (Fig. 7D, paired t-test, pFDR = 0.4), with an average increase of $43.1 \pm 20.1\%$. The lidocaine blockade did not affect the rate of 8 units in the EPL.

Lidocaine application significantly reduced the mean spontaneous activity rate of 8 units recorded in the MCL (two of which were antidromically activated) from 19.9 ± 4 Hz to 10.7 ± 2.9 Hz (Fig. 8C, paired t-test, $p = 0.0009$, pFDR = 0.01), with an average decrease of $48.9 \pm 5.8\%$. Lidocaine application increased the mean rate in 5 other units recorded in the MCL from 20.6 ± 5 Hz to 32.5 ± 5 Hz, but did not achieve statistical significance (Fig. 8D, paired t-test, $p = 0.02$, pFDR = 0.07), with an average

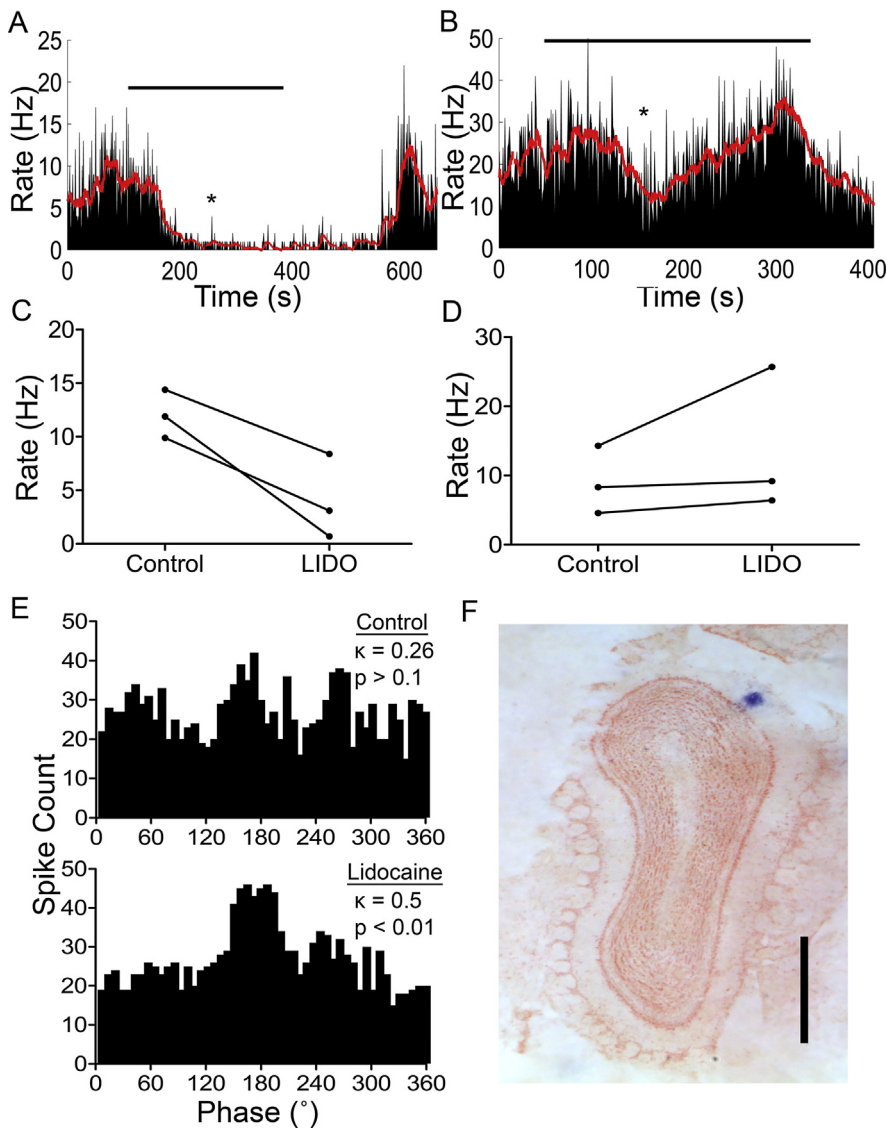


Fig. 7. External plexiform layer single-unit spontaneous activity is modulated by centrifugal fiber input. A. Representative EPL unit ratemeter showing that lidocaine (bar) decreased spontaneous activity from 11.9 Hz to 0.69 Hz, and that baseline rate measurements were stable; red trace overlay, mean rate frequency. LOT was estimated to be maximally blocked around 250 s after lidocaine application; *. B. Representative EPL unit ratemeter showing that lidocaine (bar) increased spontaneous activity from 14.3 Hz to 25.7 Hz, and that baseline rate measurements were stable; red trace overlay, mean rate frequency. LOT was estimated to be maximally blocked around 150 s after lidocaine application; *. C. LOT block did not significantly alter the spontaneous activity rate of EPL units that were classified as having decreased, $p\text{FDR} = 0.09$. D. Lidocaine application did not significantly change the spontaneous activity of EPL units that were classified as having increased, $p\text{FDR} = 0.4$. E. Sample phase histograms of a unit recorded in the EPL before and after lidocaine application. Top panel, unit activity was not entrained with respiration before lidocaine, $\kappa = 0.26$, $p > 0.1$. Bottom panel, lidocaine application resulted in significant spike entrainment, $\kappa = 0.5$, $p < 0.01$. F. Representative histological determination of recording electrode position in the external plexiform layer, blue spot. Scale bar, 1 mm.

increase of $78.8 \pm 30.7\%$. There were no mitral cell units in this study where the lidocaine blockade failed to modify the spontaneous activity.

In the GCL, lidocaine block decreased the mean rate in 7 units from 21.7 ± 7.5 Hz to 7.7 ± 3.6 Hz; however the difference was not statistically significant (Fig. 9C, paired t-test, $p = 0.04$, $p\text{FDR} = 0.09$) with an average decrease of $65.3 \pm 8.5\%$; 2 GCL units increased in

mean rate after LOT block from 4.8 ± 3.9 Hz to 7 ± 5.4 Hz (Fig. 9D) with an average increase of $64.8 \pm 22.5\%$. Lidocaine application did not affect the rate of two units recorded in the GCL. The identity of these neurons beyond the layer where the unit was recorded was not known.

A two-tailed paired t-test used to compare the rates before and after lidocaine for all recorded units, including those whose rate did not change, showed that the lidocaine blockade of centrifugal fibers in the LOT decreased the mean rate of spontaneous activity from 17.1 ± 1.8 Hz to 13.7 ± 1.8 Hz, however statistical significance was not achieved ($n = 49$, $p = 0.02$, $p\text{FDR} = 0.07$). Chi-square analysis of the bulbar neuron responses to LOT block revealed that the effects of LOT block varied significantly between layers ($\chi^2 = 13.6$, $p = 0.035$).

Additionally, the CV of inter-spike intervals and respiratory phase entrainment of unit activity were also examined. CVs of all single-unit recordings were compared using a paired t-test before and during lidocaine block; no significant differences were found. There was also no significant difference in CVs when comparing single units before and during lidocaine block in each cell layer. Units recorded in the GL whose rate did not change after lidocaine exhibited a mean decrease in CV that did not achieve significance ($p = 0.02$, $p\text{FDR} = 0.26$).

Respiratory entrainment was observed in 27% of the units recorded from all cell layers which increased to 37% of units displaying respiratory entrainment after LOT block. Lidocaine blockade had the following discrete effects: 6 units lost their entrainment after lidocaine, and 11 units became entrained after the lidocaine block. 25 units that were not entrained

before the block did not change, and 7 units that were entrained stayed synchronized after the block.

The present studies demonstrate that inhibition of tonically active centrifugal fibers of the LOT dynamically modulate the excitability of bulbar neurons in the absence of odors; the spontaneous activity of some single units recorded across all layers increased, while others decreased.

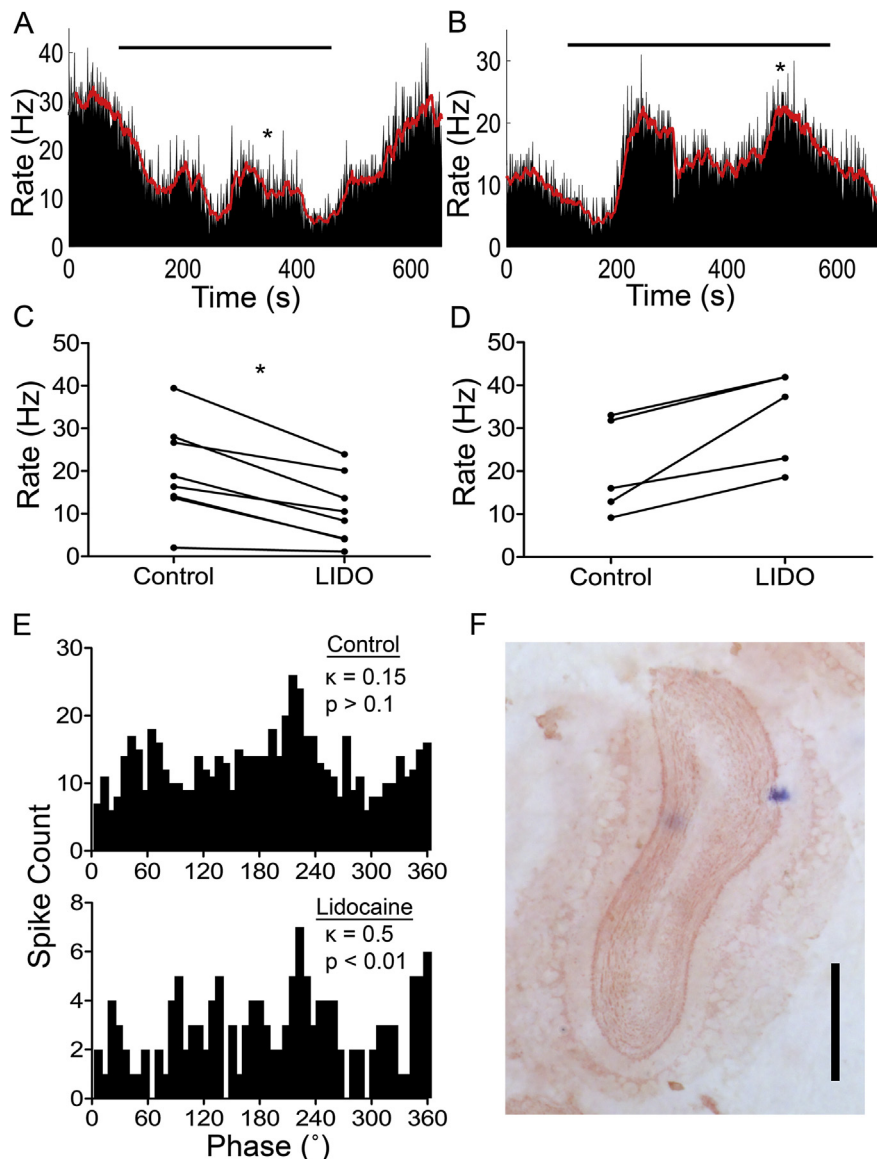


Fig. 8. Tonic centrifugal fiber input significantly enhances the single-unit spontaneous activity in the mitral cell layer. **A.** Representative MCL unit ratemeter demonstrating that lidocaine (bar) decreased spontaneous activity from 28 Hz to 13.67 Hz, and that baseline rate measurements were stable; red trace overlay, mean rate frequency. LOT was estimated to be maximally blocked around 315 s after lidocaine application, *. **B.** Representative MCL unit ratemeter showing that lidocaine (bar) increased spontaneous activity from 9.16 Hz to 18.54 Hz, and that baseline rate measurements were stable; red trace overlay, mean rate frequency. LOT was estimated to be maximally blocked around 530 s after lidocaine application; *. **C.** LOT block significantly decreased the rate of spontaneous activity of MCL units that were classified as having decreased, $pFDR = 0.01$. (*, $pFDR < 0.05$). **D.** Lidocaine application did not significantly alter the spontaneous activity rate of MCL units that were classified as having increased, $pFDR = 0.07$. **E.** Sample phase histograms of a unit in the MCL before and after lidocaine application. Top panel, unit activity was not entrained with respiration before lidocaine, $\kappa = 0.15$, $p > 0.1$. Bottom panel, unit activity was significantly entrained with respiration, $\kappa = 0.5$, $p < 0.01$. **F.** Representative histological determination of recording electrode position in the mitral cell layer, blue spot. Scale bar, 1 mm.

DISCUSSION

These experiments demonstrate that tonic activity of centrifugal fibers that travel through the LOT modifies the spontaneous activity of MOB neurons. Measurements of spontaneous activity were obtained

before and after topical lidocaine application to the LOT. The control (before) rates of spontaneous activity in this study were comparable to previous studies. For example, the mean spontaneous activity of the 9 units recorded in the GCL (18.2 ± 17.3 Hz) was comparable to, though a bit higher than the 10.3 ± 3 Hz reported by [Stacic et al. \(2011\)](#). In a study using the urethane anesthetized rat, most granule cells had no spontaneous activity and those that did had activity of less than 0.5 Hz ([Cang and Isaacson, 2003](#)). The mean spontaneous activity of the 13 units recorded in the MCL (20.2 ± 10.8 Hz) was similar to values reported by [Stacic et al. \(2011\)](#), control rate: 16 ± 5.3 Hz), [Nica et al. \(2010\)](#), control rate: 17.38 ± 8.3 Hz) and [Griff et al. \(2008\)](#), control rate: 14.7 ± 6.2 Hz). The mean rates for units recorded in the external plexiform and GLs, 16.5 ± 4.2 Hz and 18.2 ± 5.2 Hz, respectively, compare well with the values reported by [Griff et al. \(2008\)](#) of 15.9 ± 6.4 Hz and 18.9 ± 8.8 Hz. No attempt was made to identify units that were antidromically activated from the LOT, indicating that they were either mitral or tufted cells, but had no spontaneous activity.

The protocol provided for only about 3 min of baseline before applying the lidocaine so that there could be time to show the recovery from lidocaine before losing the unit. The mean time for the total of baseline, lidocaine application duration, and recovery was about 15 min (917.6 ± 362.5 s). In addition to the data recorded during the control, before lidocaine period, stability during the pre-baseline period and during the recovery were also considered when determining whether a unit's baseline was stable enough to be included in the data set.

Experiments were conducted with anesthetized adult male rats maintained at a constant anesthetic plane (see Section "Experimental procedures"). [Li et al. \(2011, 2012\)](#) compared two levels/states of chloral

hydrate anesthesia in their studies of the olfactory bulb. Our data is more similar to their EEG recordings and single-unit spontaneous activity in the high state with the lowest level of chloral hydrate. In their comparison between the anesthetized and the awake animal ([Li](#)

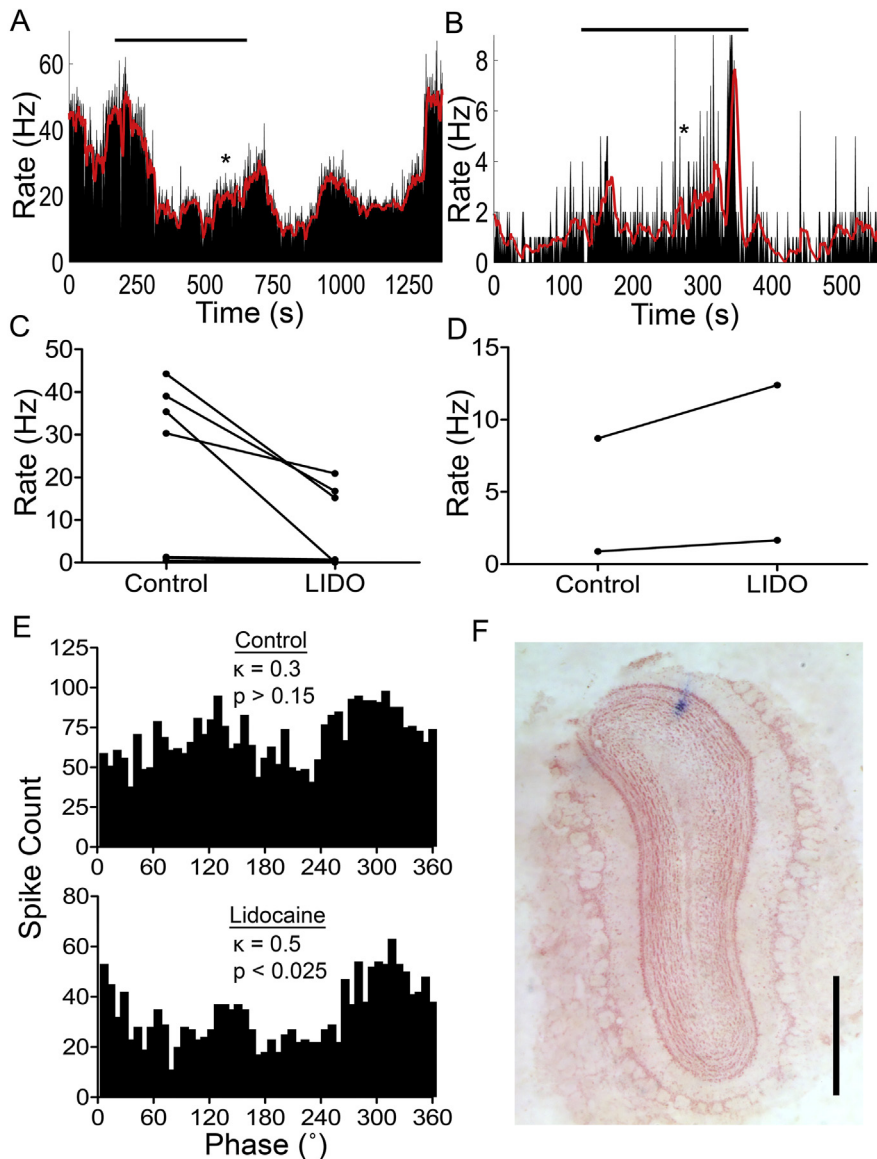


Fig. 9. Granule cell layer single-unit spontaneous activity is modulated by centrifugal fiber input. A. Representative GCL unit ratemeter showing that lidocaine (bar) decreased spontaneous activity from 39.02 Hz to 16.76 Hz, and that baseline rate measurements were stable; red trace overlay, mean rate frequency. LOT was estimated to be maximally blocked around 585 s after lidocaine application, *. B. Representative GCL unit ratemeter showing that lidocaine (bar) increased spontaneous activity from 0.88 Hz to 1.6 Hz, and that baseline rate measurements were stable; red trace overlay, mean rate frequency. LOT was estimated to be maximally blocked around 270 s after lidocaine application, *. C. LOT block did not significantly alter the spontaneous activity rate of GCL units that were classified as having decreased, pFDR = 0.09. D. Mean increase of GCL unit spontaneous activity after lidocaine application. E. Sample phase histograms of a GCL unit before and after lidocaine. Top panel, unit activity was not entrained with respiration before lidocaine, $\kappa = 0.3$, $p > 0.15$. Bottom panel, unit activity was significantly entrained after lidocaine, $\kappa = 0.5$, $p < 0.025$. F. Representative histological determination of recording electrode position in the granule cell layer, blue spot. Scale bar, 1 mm.

et al., 2012), our EEG data more closely resemble the local field potentials recorded near the end of the recovery period, more than 60 min after injecting the chloral hydrate. No single-unit data were shown in that paper. Rinberg et al. (2006) compared spontaneous activity between awake and ketamine/xylazine anesthetized mice, raising the question of the relevance of studying spontaneous activity in an anesthetized preparation.

The single-unit recordings in the present and previous studies from our lab are more consistent with the rate and temporal pattern of the awake mice of the Rinberg et al. study. Furthermore, recent experiments from our lab (Rohrbaugh & Griff, unpublished data) show additional ketamine/xylazine anesthesia applied to our *in vivo* preparation caused a noticeably sharp inhibition of spontaneously generated spikes in bulbar neurons, consistent with the anesthetic effects observed by Rinberg et al. (2006). These recent results suggest that the changes in spontaneous activity observed by Rinberg et al. could be ketamine/xylazine specific. Thus, chloral hydrate anesthesia at a plane where a hard pinch desynchronizes the EEG without eliciting a withdrawal response is a reasonable protocol for studying spontaneous activity. Deeper anesthetic levels can cause slow oscillations of the spontaneous activity (Jiang et al., 1996). Maintaining a constant level of anesthesia through the use of EEG monitoring, is a key aspect of this study.

Because centrifugal fibers that project from olfactory cortices, basal forebrain, reticular formation, and pons to the MOB form two major pathways through the AON and the LOT which are in close proximity (Laaris et al., 2007), the efficacy and selectivity of the topical lidocaine LOT application is another important aspect of the experimental design. Lidocaine-soaked cotton balls were selected for use to block conduction because they could be visually localized to the LOT (Fig. 2), and because lidocaine effectively inhibited LOT-evoked field potentials (Fig. 3) while being quickly reversible by ACSF washout so that spontaneous activity before, during, and after the application could be measured. Additionally, we demonstrate that the topical lidocaine application was selective for the LOT, while not inhibiting the

AON or the MOB (Fig. 3). Using a topical application, several units could be studied in the same animal; this is an important difference from studies where the LOT was surgically interrupted (e.g. Chaput, 1983). Furthermore, the recovery time in our study (mean 416.1 s) is considerable shorter than the 30- to 40-min recovery observed with stereotaxic injections (Tehovnik and Sommer, 1997; Boehnke and Rasmusson, 2001).

For every unit, control field potentials from either the AON, ON, or ONL at the rostral MOB were recorded at the time when the blockade of the LOT was assessed. Thus, the spread of lidocaine was ascertained for each and every unit at the time when the LOT was blocked by lidocaine. In addition, further off-target effects of lidocaine application were evaluated by measuring compound action potentials evoked from a site rostral to the lidocaine block (Fig. 4). For these compound action potential experiments, the mean contact time for the lidocaine was 310 s, and this is comparable to the mean application time of 353 s. If the longest application time is removed, this mean drops to 336 s. Furthermore, Martin (1991) showed that the maximum spread of lidocaine occurred at 20 min after application; in our experiments the lidocaine was removed and rinsed before 20 min.

The observed effects of the lidocaine application were potentially influenced by the exact placement of the lidocaine-containing cotton ball on the LOT, the total volume of lidocaine that made contact with the LOT, and the location of the recording electrode relative to the fibers that were blocked by the lidocaine. While the discreet application of lidocaine in the present study provided high specificity and reversibility of the LOT blockade, it also made it unlikely that all centrifugal fibers contained by the LOT were inhibited by the lidocaine. The discreet application strategy and the resulting incomplete block of the LOT could be responsible for a lack of a response to lidocaine in some single-unit recordings.

Blocking tonic centrifugal activity through the LOT increased or decreased the activity of some neurons, and had no effect on others. The subpopulation of single units whose spontaneous activity was unaltered by lidocaine application potentially includes units that are innervated by centrifugal fibers in the LOT that are silent at rest, or by centrifugal fibers that did not make contact with the lidocaine application and therefore were still active. Additionally, it is likely that some MOB cells do not receive centrifugal input via the LOT but rather, only from the AON or piriform cortex (Carson, 1984; Laaris et al., 2007).

The most direct explanation for the observed decrease in spontaneous activity after lidocaine application, the most common change, is that a steady-state excitatory drive onto bulbar neurons was blocked. Inhibition of excitatory neurotransmitter release onto bulbar neurons which would result in decreased spontaneous action potential generation. Another way to decrease spontaneous activity is to reduce GABA release onto other GABAergic interneurons, reducing disinhibition. This is consistent with prior studies which reported that the average membrane potential of mitral cells in LOT-lesioned animals was more hyperpolarized than control animals, possibly because these cells were more inhibited in the absence of centrifugal input from the LOT (Phillips et al., 2012). LOT block increased spontaneous activity in 24% of the units in this study. An increase in spontaneous activity

could result from decreased release of GABA onto the recorded unit.

Our findings in combination with prior reports of tonic neurotransmission in the MOB strongly support the hypothesis that centrifugal fibers of the LOT are active during the steady-state and tonically release neurotransmitters onto bulbar neurons. As such, neurons in the piriform cortex have been shown to be spontaneously active (Sanchez-Vives et al., 2008), as have been neurons in the medial part of the HDB (Linster and Hasselmo, 2000). Decreases in both choline acetyltransferase and acetylcholinesterase levels in the MOB after olfactory peduncle sectioning has been previously documented; this suggests a resultant decrease in cholinergic input to the MOB by centrifugal fibers (Godfrey et al., 1980). Additionally, Shute and Lewis (1967) observed an increase in acetylcholinesterase levels in the LOT at a location that was caudal to a lesion made at the base of the olfactory peduncle. Lesioning of the HDB also results in a decrease in acetylcholinesterase and choline acetyltransferase staining that is directly proportional to the size and extent of the HDB lesion (Davis and Macrides, 1981). This suggests that tonic ACh release from centrifugal fibers projecting to the MOB from the HDB occurs during the steady-state. The same lesioned animals from the Godfrey et al. (1980) experiments also exhibited a prominent decrease in glutamate and GABA levels in the MOB. Taken together, these studies support our hypothesis that blocking action potential conduction in the LOT reduces tonic neurotransmitter release in the MOB that could increase or decrease the spontaneous activity of bulbar neurons.

Temporal patterns of action potentials are an important feature of olfactory neurons, including their spontaneous activity (Yu et al., 2004; Griff et al., 2008; Favela et al., 2016). In the present paper, the coefficient of variability (CV) was used as an index of time-dependent bursting. A high CV indicates time-dependent bursts of action potentials, and a lower CV indicates that the unit's spike discharge is more regular. One group of units recorded in the GL exhibited a decrease in CV associated with lidocaine inhibition of LOT centrifugal fibers, though the mean rate of activity of these units did not change significantly. External tufted cells in the GL have been shown to exhibit intrinsic bursting whose frequency is voltage-dependent and can be modified by synaptic input (Hayar et al., 2004). The specific class of units recorded in the GL whose CV changed in the present study was not known. However, the possibility remains that neuromodulatory neurotransmission from tonic centrifugal fiber activity could alter the ionic conductances which have been shown to regulate juxtglomerular neuron bursting (Liu and Shipley, 2008).

Top-down modulation can influence both neuronal firing rates and the temporal structure of neural responses, including synchronization of spike discharge and oscillations in spontaneous, ongoing activity (e.g. Engel et al., 2001). Ongoing rhythms could organize selective attention to relevant stimuli, such as visual signals, even before the stimulus is presented (Tsodyks

et al., 1999). The temporal pattern of spontaneous activity measured by the CV can be modulated. For example, blocking input from the medial Raphe nucleus to the hippocampus increases the rate and regularity of hippocampal neurons (Vinogradova et al., 1999).

Another important temporal feature of bulbar neuron spontaneous activity is the entrainment of spontaneous spikes with the respiratory cycle, which is driven by some combination of ON activity, centrifugal input, and/or intrinsic bulbar circuit activity (Laurent, 2002; Buonviso et al., 2006; Rothermel et al., 2014). Respiratory entrainment of spontaneous spikes in a portion of recorded units in the present study was affected by blocking centrifugal fiber activity. Respiratory entrainment was enhanced by tonic centrifugal input in 6 recorded units, while in 11 units, entrainment was dampened. The respiratory entrainment of more than half of all recorded units was unaffected by blocking centrifugal input. Prior studies have demonstrated that mitral and tufted neuron spike entrainment with respiration can also be dependent on nasal airflow (Phillips et al., 2012). Nonetheless, the effect of tonic input from centrifugal fibers seems to have an additional role in regulating respiratory entrainment.

The action of tonically released neurotransmitters from centrifugal fibers is likely the same as the action caused by stimulation of centrifugal input sources, with similar effects on bulbar neuron excitability (Nickell and Shipley, 1988). Centrifugal fibers arising from the primary olfactory cortex to granule cells are glutamatergic and a small portion travels through the LOT (Price and Powell, 1970a,c; Davis and Macrides, 1981; Ennis et al., 2007; Laaris et al., 2007) and can provide disynaptic inhibition of mitral cells (Boyd et al., 2012). The HDB contains both cholinergic and GABAergic neurons (Zaborszky et al., 1986), and electrical or optogenetic stimulation of the HDB has been shown to elicit both increases and decreases in bulbar neuron spontaneous activity (Ma and Luo, 2012; Zhan et al., 2013). On the other hand, direct optogenetic stimulation of cholinergic neurons in the MOB increased spontaneous activity of presumed mitral/tufted cells (Rothermel et al., 2014). Note that the control spontaneous activity rates in Ma and Luo (2012) and the Rothermel et al. (2014) were very low compared to the present study (rat) and low in comparison to a previous study in mouse (Mast and Griff, 2007). These conflicting results could reflect different pathways innervating the MOB from the HDB or the different methods of stimulating the HDB.

CONCLUSIONS

The present study identifies steady-state centrifugal fiber activity as a key regulator of spontaneous activity of MOB neurons, providing both dampening and enhancing influences on their excitability. However, further experiments will be critical to determine the influence of specific sources of centrifugal fibers. Olfactory-specific regions of the cortex have been shown to be spontaneously active, projecting centrifugal fibers to both contralateral and ipsilateral MOBs (Mori et al., 1979; Linster and Hasselmo, 2000; Sanchez-Vives

et al., 2008) via fibers that make up the anterior commissure, or through the LOT. Interestingly, AON centrifugal axons have been shown to have diverse functionality by supplying ipsilateral centrifugal excitation and contralateral inhibition to bulbar neurons to allow for left–right detection of odorants (Kikuta et al., 2010). This suggests that the tonic activity of centrifugal fibers arising from the AON or the HDB could be functionally distinct compared to the heterogeneous bottleneck of centrifugal fibers in the LOT. Therefore, further study will be necessary to determine the respective influences of tonically active centrifugal fibers originating from the AON or HDB compared to the LOT by selectively inhibiting each region of interest while measuring spontaneous activity.

Acknowledgments—The authors would like to thank Ms. Madeleine Lansberry, Ms. Alyssa Rohrbaugh, Mr. Sadik Silbak, Mr. Udhay Joshi, and Mr. Timothy Smile for their assistance during recording sessions. Additionally, Dr. Mark L. Baccei and Mr. Arnold Gutierrez provided helpful comments during the preparation of this manuscript. This work was supported by grants from the University of Cincinnati Department of Biological Sciences, and from the University Research Council at the University of Cincinnati awarded to ERG; and grants from the University Research Council-Graduate Student Research Fellowship at the University of Cincinnati and from the Weiman-Wendel-Benedict fund at the University of Cincinnati Department of Biological Sciences awarded to NCF.

REFERENCES

- Boehnke SE, Rasmusson DD (2001) Time course and effective spread of lidocaine and tetrodotoxin delivered via microdialysis: an electrophysiological study in cerebral cortex. *J Neurosci Methods* 105:133–141.
- Boyd AM, Sturgill JF, Poo C, Isaacson JS (2012) Cortical feedback control of olfactory bulb circuits. *Neuron* 76:1161–1174.
- Brunjes PC, Illig KR, Meyer EA (2005) A field guide to the anterior olfactory nucleus (cortex). *Brain Res Brain Res Rev* 50:305–335.
- Buonviso N, Amat C, Litaudon P (2006) Respiratory modulation of olfactory neurons in the rodent brain. *Chem Senses* 31:145–154.
- Cang J, Isaacson JS (2003) In vivo whole-cell recording of odor-evoked synaptic transmission in the rat olfactory bulb. *J Neurosci* 23:4108–4116.
- Carson KA (1984) Quantitative localization of neurons projecting to the mouse main olfactory bulb. *Brain Res Bull* 12:629–663.
- Chaput M (1983) Effects of olfactory peduncle sectioning on the single unit responses of olfactory bulb neurons to odor presentation in awake rabbits. *Chem Senses* 8:161–177.
- Chaput MA, Buonviso N, Berthommier F (1992) Temporal patterns in spontaneous and odour-evoked mitral cell discharges recorded in anaesthetized freely breathing animals. *Eur J Neurosci* 4:813–822.
- Ciombor KJ, Ennis M, Shipley MT (1999) Norepinephrine increases rat mitral cell excitatory responses to weak olfactory nerve input via alpha-1 receptors in vitro. *Neuroscience* 90:595–606.
- Davis BJ, Macrides F (1981) The organization of centrifugal projections from the anterior olfactory nucleus, ventral hippocampal rudiment, and piriform cortex to the main olfactory bulb in the hamster: an autoradiographic study. *J Comp Neurol* 203:475–493.
- Devore S, Linster C (2012) Noradrenergic and cholinergic modulation of olfactory bulb sensory processing. *Front Behav Neurosci* 6:52.
- Engel AK, Fries P, Singer W (2001) Dynamic predictions: oscillations and synchrony in top down processing. *Nature Rev Neurosci* 2:704–716.

- Ennis M, Hayar A (2008) Physiology of the main olfactory bulb. In: Firestein S, Beauchamp G, editors. *The senses: a comprehensive reference*, vol. 4. San Diego, CA: Academic Press. p. 641–686.
- Ennis MH, Hamilton KA, Hayar A (2007) Neurochemistry of the main olfactory system. In: Lajtha A, Johnson DA, editors. *Handbook of neurochemistry and molecular neurobiology*. Verlag, Berlin, Heidelberg: Springer. p. 139–182.
- Favela LH, Coey CA, Griff ER, Richardson MJ (2016) Fractal analysis reveals subclasses of neurons and suggests an explanation of their spontaneous activity. *Neurosci Lett* 626:54–58.
- Fletcher ML, Chen WR (2010) Neural correlates of olfactory learning: Critical role of centrifugal neuromodulation. *Learn Mem* 17:561–570.
- Godfrey DA, Ross CD, Herrmann AD, Matschinsky FM (1980) Distribution and derivation of cholinergic elements in the rat olfactory bulb. *Neuroscience* 5:273–292.
- Gray CM, Skinner JE (1988) Centrifugal regulation of neuronal activity in the olfactory bulb of the waking rabbit as revealed by reversible cryogenic blockade. *Exp Brain Res* 69(2):378–386.
- Griff ER, Mafhouz M, Perrut A, Chaput MA (2008) Comparison of identified mitral and tufted cells in freely breathing rats: I. Conduction velocity and spontaneous activity. *Chem Senses* 33:779–792.
- Hayar A, Karnup S, Ennis M, Shipley MT (2004) External tufted cells: a major excitatory element that coordinates glomerular activity. *J Neurosci* 24:6676–6685.
- Inokuchi A, Restrepo JP, Snow Jr JB (1987) Effect of stimulation of the horizontal limb of the diagonal band on rat olfactory bulb neuronal activity. *Am J Otolaryngol* 8:205–210.
- Jeune LH, Aubert I, Jourdan F, Quirion R (1995) Comparative laminar distribution of various autoradiographic cholinergic markers in adult rat main olfactory bulb. *J Chem Neuroanat* 9(2):99–112.
- Jiang M, Griff ER, Ennis M, Zimmer LA, Shipley MT (1996) Activation of locus coeruleus enhances the responses of olfactory bulb mitral cells to weak olfactory nerve input. *J Neurosci* 16:6319–6329.
- Kikuta S, Sato K, Kashiwadani H, Tsunoda K, Yamasoba T, Mori K (2010) From the Cover: neurons in the anterior olfactory nucleus pars externa detect right or left localization of odor sources. *Proc Natl Acad Sci USA* 107:12363–12368.
- Kiselycznyk CL, Zhang S, Linster C (2006) Role of centrifugal projections to the olfactory bulb in olfactory processing. *Learn Mem* 13:575–579.
- Laaris N, Puche A, Ennis M (2007) Complementary postsynaptic activity patterns elicited in olfactory bulb by stimulation of mitral/tufted and centrifugal fiber inputs to granule cells. *J Neurophysiol* 97:296–306.
- Lai J, Porreca F, Hunter JC, Gold MS (2004) Voltage-gated sodium channels and hyperalgesia. *Annu Rev Pharmacol Toxicol* 44:371–397.
- Laurent G (2002) Olfactory network dynamics and the coding of multidimensional signals. *Nat Rev Neurosci* 3:884–895.
- Leo JMC, Brunjes PC (2003) Neonatal focal denervation of the rat olfactory bulb alters cell structure and survival: a Golgi, Nissl and confocal study. *Dev Brain Res* 140(2):277–286.
- Li A, Gong L, Xu F (2011) Brain-state-independent neural representation of peripheral stimulation in rat olfactory bulb. *Proc Natl Acad Sci USA* 108:5087–5092.
- Li A, Zhang L, Liu M, Gong L, Liu Q, Xu F (2012) Effects of Different Anesthetics on Oscillations in the Rat Olfactory Bulb. *J Am Assoc Lab Anim Sci* 51:458–463.
- Linster C, Hasselmo ME (2000) Neural activity in the horizontal limb of the diagonal band of Broca can be modulated by electrical stimulation of the olfactory bulb and cortex in rats. *Neurosci Lett* 282(3):157–160.
- Liu S, Shipley MT (2008) Multiple conductances cooperatively regulate spontaneous bursting in mouse olfactory bulb external tufted cells. *J Neurosci* 28:1625–1639.
- Lund U, Agostinelli C (2012) *CircStats: circular statistics*. In: Jammalamedaka SR, SenGupta A, editors. *Topics in circular statistics* (2001). River Edge, NJ: World Sci. <https://CRAN.R-project.org/package=CircStats>.
- Ma M, Luo M (2012) Optogenetic activation of basal forebrain cholinergic neurons modulates neuronal excitability and sensory responses in the main olfactory bulb. *J Neurosci* 32:10105–10116.
- Markopoulos F, Rokni D, Gire DH, Murthy VN (2012) Functional properties of cortical feedback projections to the olfactory bulb. *Neuron* 76:1175–1188.
- Martin JH (1991) Autoradiographic estimation of the extent of reversible inactivation produced by microinjection of lidocaine and muscimol in the rat. *Neurosci Lett* 127:160–164.
- Mast TG, Griff ER (2007) The effects of analgesic supplements on neural activity in the main olfactory bulb of the mouse. *Comp Med* 57:167–174.
- Matsutani S (2010) Trajectory and terminal distribution of single centrifugal axons from olfactory cortical areas in the rat olfactory bulb. *Neuroscience* 169:436–448.
- Matsutani S, Yamamoto N (2008) Centrifugal innervation of the mammalian olfactory bulb. *Anat Sci Int* 83:218–227.
- McLean JH, Shipley MT (1987) Serotonergic afferents to the rat olfactory bulb: I. Origins and laminar specificity of serotonergic inputs in the adult rat. *J Neurosci* 7:3016–3028.
- Mori K, Satou M, Takagi SF (1979) Axonal projection of anterior olfactory nuclear neurons to the olfactory bulb bilaterally. *Exp Neurol* 64:295–305.
- Nagayama S, Enerva A, Fletcher ML, Masurkar AV, Igarashi KM, Mori K, Chen WR (2010) Differential axonal projection of mitral and tufted cells in the mouse main olfactory system. *Front Neural Circuits*. <http://dx.doi.org/10.3389/fncir.2010.00120>.
- Nica R, Matter SF, Griff ER (2010) Physiological evidence for two classes of mitral cells in the rat olfactory bulb. *Brain Res* 1358:81–88.
- Nickell WT, Shipley MT (1988) Neurophysiology of magnocellular forebrain inputs to the olfactory bulb in the rat: frequency potentiation of field potentials and inhibition of output neurons. *J Neurosci* 8:4492–4502.
- Niedworok CJ, Schwarz I, Ledderose J, Giese G, Conzelmann KK, Schwarz MK (2012) Charting monosynaptic connectivity maps by two-color light-sheet fluorescence microscopy. *Cell Rep* 2:1375–1386.
- Omana-Zapata I, Khabbaz MA, Hunter JC, Bley KR (1997) QX-314 inhibits ectopic nerve activity associated with neuropathic pain. *Brain Res* 771:228–237.
- Paxinos G, Watson C (1998) *The Rat Brain in Stereotaxic Coordinates*. San Diego: Academic Press.
- Persaud N, Strichartz GR (2002) Micromolar lidocaine selectively blocks propagating ectopic impulses at a distance from their site of origin. *Pain* 99:333–340.
- Phillips ME, Sachdev RN, Willhite DC, Shepherd GM (2012) Respiration drives network activity and modulates synaptic and circuit processing of lateral inhibition in the olfactory bulb. *J Neurosci* 32:85–98.
- Pinching AJ, Powell TPS (1972) The termination of centrifugal fibres in the glomerular layer of the olfactory bulb. *J Cell Sci* 10:621–635.
- Pompeiano M, Palacios JM, Mengod G (1994) Distribution of the serotonin 5-HT₂ receptor family mRNAs: comparison between 5-HT_{2A} and 5-HT_{2C} receptors. *Mol Brain Res*.
- Price JL, Powell TP (1970a) An electron-microscopic study of the termination of the afferent fibres to the olfactory bulb from the cerebral hemisphere. *J Cell Sci* 7:157–187.
- Price JL, Powell TP (1970b) An experimental study of the origin and the course of the centrifugal fibres to the olfactory bulb in the rat. *J Anat* 107:215–237.
- Price JL, Powell TP (1970c) The synaptology of the granule cells of the olfactory bulb. *J Cell Sci* 7:125–155.
- R Core Team (2016) *R: A language and environment for statistical computing*. Vienna, Austria: R Foundation for Statistical Computing.
- Rinberg D, Koulakov A, Gelperin A (2006) Sparse odor coding in awake behaving mice. *J Neurosci* 26:8857–8865.

- Rothermel M, Carey RM, Puche A, Shipley MT, Wachowiak M (2014) Cholinergic inputs from Basal forebrain add an excitatory bias to odor coding in the olfactory bulb. *J Neurosci* 34:4654–4664.
- Sanchez-Vives MV, Descalzo VF, Reig R, Figueroa NA, Compte A, Gallego R (2008) Rhythmic spontaneous activity in the piriform cortex. *Cereb Cortex* 18:1179–1192.
- Shute CCD, Lewis PR (1967) The ascending cholinergic reticular system: neocortical, olfactory and subcortical projections. *Brain* 90:497–512.
- Stacic J, Suchanek JM, Ziegler GP, Griff ER (2011) The source of spontaneous activity in the main olfactory bulb of the rat. *PLoS One* 6:e23990.
- Tehovnik EJ, Sommer MA (1997) Effective spread and timecourse of neural inactivation caused by lidocaine injection in monkey cerebral cortex. *J Neurosci Methods* 74:17–26.
- Tsodyks M, Kanet T, Grinvald A, Arieli A (1999) Linking spontaneous activity of single cortical neurons and the underlying functional architecture. *Science* 286:1943–1946.
- Vinogradova OS, Kitchigina VF, Rudina TA, Zenchenko KI (1999) Spontaneous activity and sensory responses of hippocampal neurons during persistent theta-rhythm evoked by midline raphe nucleus blockade in rabbit. *Neuroscience* 94:745–753.
- Yu CR, Power J, Barnea G, O'Donnell S, Brown HEV (2004) Spontaneous neural activity is required for the establishment and maintenance of the olfactory sensory map. *Neuron* 42(4):553–566.
- Zaborszky L, Carlsen J, Brashear HR, Heimer L (1986) Cholinergic and GABAergic afferents to the olfactory bulb in the rat with special emphasis on the projection neurons in the nucleus of the horizontal limb of the diagonal band. *J Comp Neurol* 243:488–509.
- Zhan X, Yin P, Heinbockel T (2013) The basal forebrain modulates spontaneous activity of principal cells in the main olfactory bulb of anesthetized mice. *Front Neural Circuits* 7:148.

(Received 8 July 2016, Accepted 8 February 2017)
(Available online 16 February 2017)